JOURNAL OF MATERIALS SCIENCE 29 (1994) 449–455

Shape memory effect by constant-stress ageing in Ti–50.5 at % Ni alloy

R. D. JEAN
Materials Research Laboratory, Industrial Technology Research Institute, Hsinchu 31015, Taiwan
C. T. HU
Department of Materials Science and Engineering, National Tsing Hua University, Hsinchu 30043, Taiwan

In 300–500 °C ageing, the H_V value and M_s temperature are strongly affected by the ageing time. The M_s temperature was found to drop during early ageing and then to increase. The H_V value was found to increase during early ageing and then to decrease. However, precipitation hardening is one of the variables that affect the M_s temperature. The precipitates were lined up in a single preferred orientation during the constraint ageing condition. The precipitates with preferred orientation caused a shear stress field which improved the martensitic transformation. The result is that the stress required to induce martensite decreases and the M_s temperature increases.

1. Introduction

Among shape memory alloys, Ni–Ti alloys of near-equiatomic composition have been used for various commercial applications, since they have good mechanical properties and the well-known shape memory effect [1, 2]. Recently, several investigations have been conducted in order to further improve their shape memory effect, and some of the improved methods have adopted the same approach: making use of precipitates in Ni-rich alloys [3–5]. To this end, many investigations have been made in order to establish the influence of the precipitates. It has been observed that when a low ageing temperature is used, the martensitic transformation starting temperature M_s undergoes several changes during the course of ageing. The M_s temperature was found to drop dramatically early in ageing, and then to rapidly increase. To give more insight into this phenomenon, this paper establishes the T–T–T curves for several precipitate phases and also studies the effect of precipitation hardening on M_s.

In 1984, Nishida and Honma [6, 7] studied the constraint ageing effect on the Ni–Ti shape memory alloy and found that the constraint-ageing alloy generates an all-round shape memory (ARSM) effect. It was reported that surface strains between the matrix and $Ti_{11}Ni_{14}$ precipitates relate to this effect, and that each grain in the ARSM alloy has only a single variant of martensite. The second part of this paper picks up this particular subject and documents the effect of constraint ageing on both M_s and the yield stress recorded in our experiments.

2. Experimental procedure

Material with a nominal composition of Ti–50.5 at % Ni was prepared from 99.9% electrolytic Ti and Ni in a high-frequency vacuum induction furnace (Leybold–Heraeus model IS8/III) with a graphite crucible. The ingot was homogenization-treated at 1000 °C for 24 h, then hot-rolled to plates of a thickness of 1.5–2 mm with intermediate annealing. Plate-type test specimens with gauge length 25 mm were sectioned from the rolled plates and solution-treated at 1000 °C for 0.5 h after being encapsuled in an evacuated quartz tube, followed by quenching into cold water. They were divided into several groups and aged at 300, 400 or 500 °C in a salt bath for various periods, while they were subjected either to no constraint or to a constant tensile stress of 30, 40, 50 or 60 MPa. The facility to provide constant-stress loading is schematically drawn in Fig. 1. Tensile tests were carried out at room temperature with an Instron model 8031 testing machine at a strain rate of 4 $\times 10^{-4}$ s^{-1}. The M_s temperature was measured using

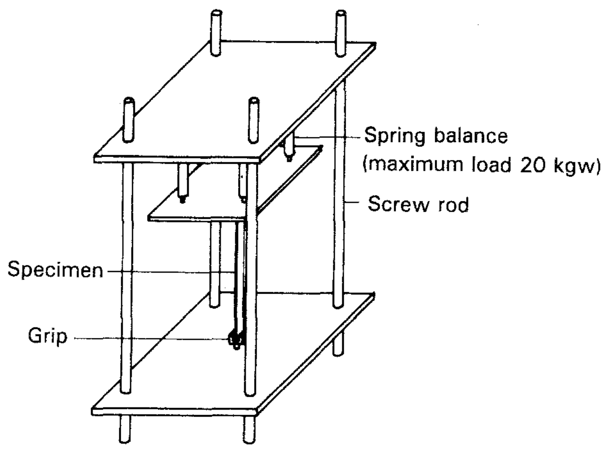

Figure 1 Schematic illustration of constant-stress loading.

a four-probe electrical resistivity measurement technique. It was observed that $M_s \simeq -25\,°C$ for the solution-treated specimens.

The investigations of precipitates during ageing with or without constraint stress were conducted by X-ray diffraction and TEM. X-ray diffraction analysis was carried out on a Rigaku X-ray diffractometer system (Geigerflex D/max-B) having a copper target

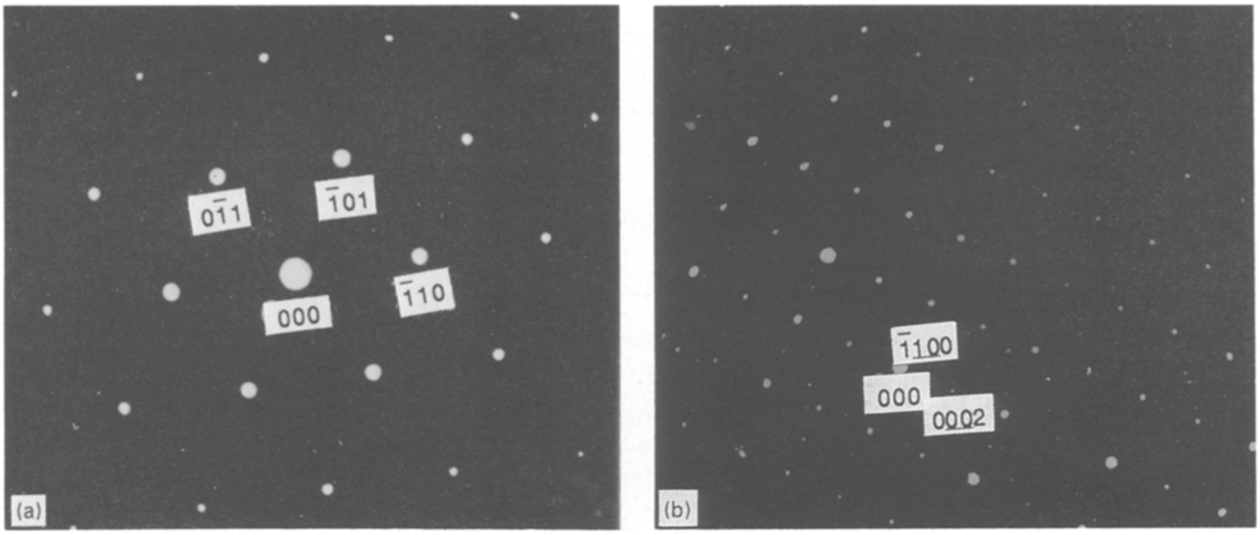

Figure 2 Electron diffraction pattern obtained from the matrix.

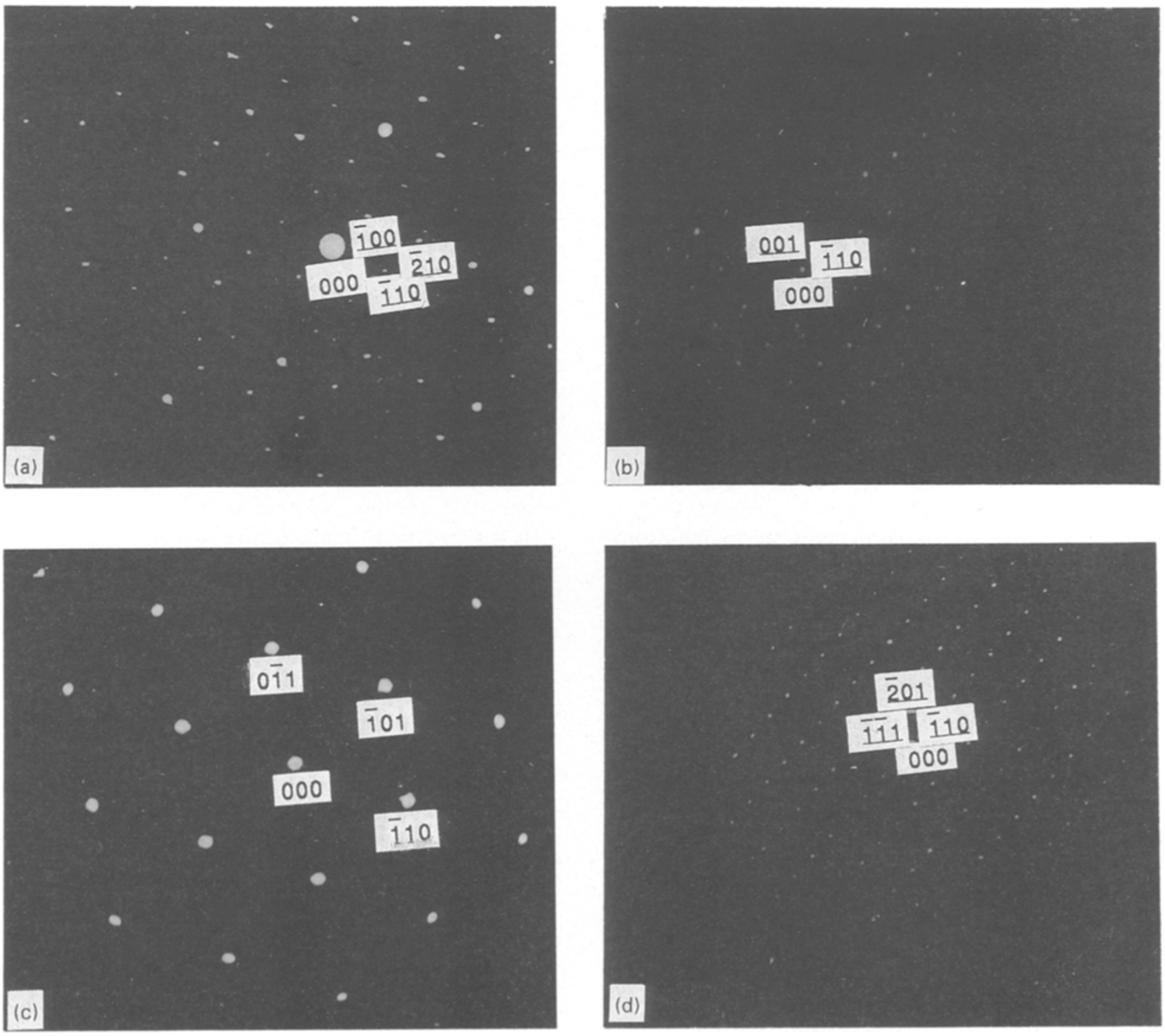

Figure 3 SADPs of specimens after ageing treatment: (a) 300 °C/15 min, (b) 300 °C/1 h, (c) 400 °C/1 h, (d) 500 °C/15 min.

and step-scan mode. Thin foils for TEM examination were prepared by using a double-jet electropolisher with an electrolyte of 25% sulphuric acid and 75% methyl alcohol. Electron microscopic studies were performed with a Jeol 200CX STEM operated at 160 kV. Hardness tests were carried out by using a microVickers tester with 500 g load at room temperature. For each specimen, the average hardness value was taken from at least five test readings.

3. Results and discussion

3.1. Investigation of precipitates

After the specimens were examined for their microstructure, solution-treated and water-quenched, X-ray diffractometry and TEM confirmed the existence of a fully B2-ordered parent phase as shown in Fig. 2. TEM observations indicate that the selected area diffraction patterns (SADPs) of specimens after any one of the 300 °C/15 min, 300 °C/1 h, 400°C/1h and 500 °C/15 min treatments have superlattice spots of the rhombohedral $Ti_{11}Ni_{14}$ precipitate (Fig. 3.). Fig. 3c shows that the orientation relationships between B2 parent phase and $Ti_{11}Ni_{14}$ precipitate phase in the 400 °C/1 h aged specimen are $(1\,1\,0)_{Ti_{11}Ni_{14}}//(3\,2\,1)_{B2}$ and $[1\,1\,1]_{Ti_{11}Ni_{14}}//[1\,1\,1]_{B2}$. The crystal structure is determined to be rhombohedral with $a_0 = 0.661$ nm, $\alpha = 113.65$ °, which matches previous observations reported in the literature [8]. Monoclinic Ti_2 Ni_3 and h.c.p. $TiNi_3$ precipitates are observed in higher ageing-level specimens, i.e. 500 °C/1 h and 500 °C/20 h, respectively. Their TEM diffraction patterns are shown in Fig. 4. In addition, the transformation sequence of precipitates in Ni-rich TiNi SMA, i.e. $Ti_{11}Ni_{14}$ (R) → Ti_2Ni_3(M) → $TiNi_3$(H), is the same as that reported by Nishida *et al.* [9] using the STEM/EDX technique.

When the precipitate amount is small, X-ray diffraction cannot detect the precipitate diffraction peak and the initial product, $Ti_{11}Ni_{14}$, will not be detected by X-ray diffraction. It is established that a 500 °C/214–274 min ageing treatment will produce the phase transition from $Ti_2Ni_3$to $TiNi_3$, as shown in Fig. 5. This appears in X-ray diffraction as the gradual

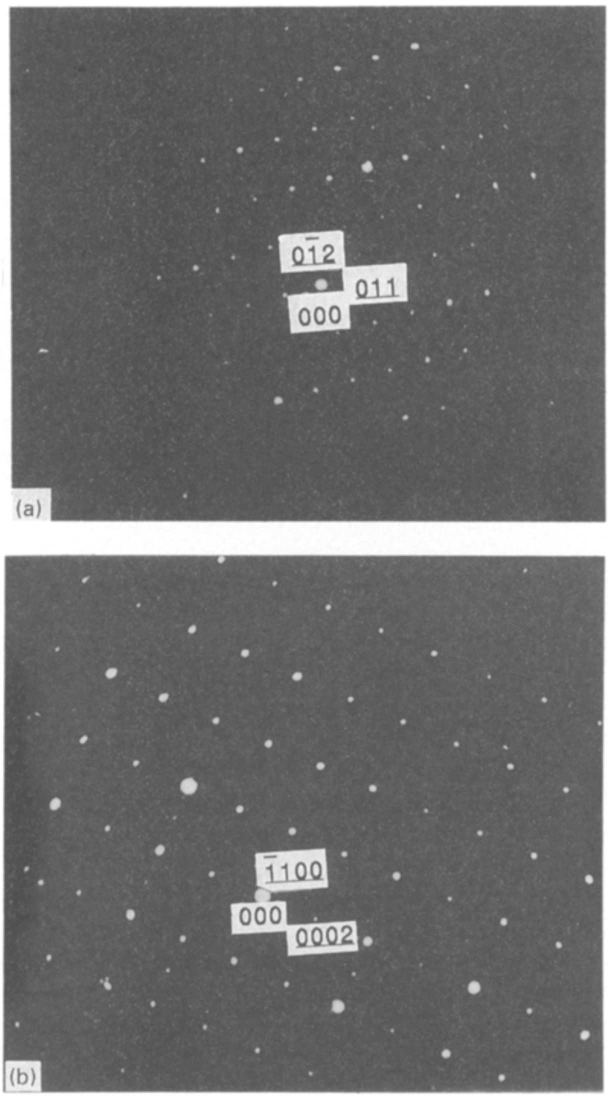

(b)

Figure 4 SADPs of specimens after ageing treatment: (a) 500 °C/1 h, (b) 500 °C/20 h.

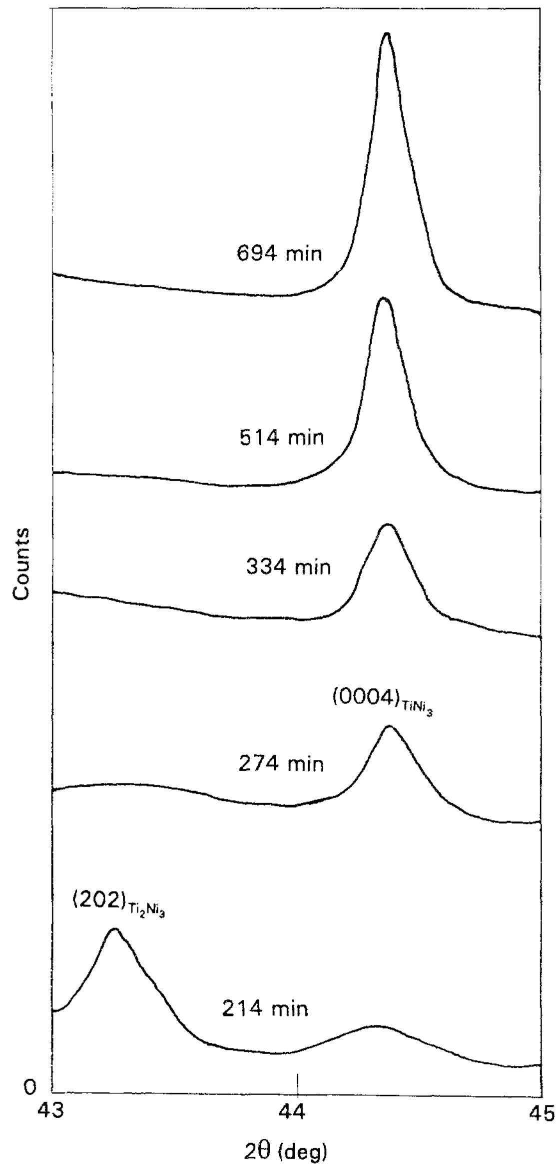

Figure 5 X-ray diffraction peak change during different ageing times at 500 °C.

disappearance of the Ti_2Ni_3 peak and the formation of a sharper $TiNi_3$ peak. X-ray diffraction also clearly shows that the precipitates transform from Ti_2Ni_3 to $TiNi_3$. Additionally, from the X-ray results, 600 °C/12 h specimens do not have any precipitate peak. A T–T–T diagram of precipitate transformation can therefore, be constructed with the above results, as illustrated in Fig. 6.

Fig. 7 shows a dark-field image of a specimen after 300 °/15 min ageing treatment without constraint stress; the precipitates are randomly distributed. Fig. 8 shows dark-field images of 50 MPa constraint-aged specimens, showing that the precipitates are lined up in a single preferred orientation.

3.2. The ageing effect on Vickers hardness

For precipitation hardening to occur, the precipitate must be coherent with the matrix. The coherent precipitate produces a strain field in the matrix and a further increase in hardness due to the extra stress required to move dislocations through the precipitate and the surrounding strain zones. Fig. 9 shows the curves for Vickers hardness corresponding to various ageing conditions. For 300 and 400 °C ageing treatments a distinct peak in hardness occurs. The hardness continues to increase with increasing ageing time and reaches a maximum when the precipitates enter the stage of critical dispersion. The harness decreases after the critical ageing time, since it means that the specimen is now over-aged; the precipitates gradually coarsen and the coherent strain surrounding the precipitates is gradually lost. The 500 °C curve has the same tendency but since it becomes over-aged shortly after ageing begins due to the raised temperature, the hardness peak is indistinct. In the case of 500 °C, coherency is not a factor and the trend of M_s is indicated by the content of Ni in the matrix: as the content falls, the M_s temperature increases throughout.

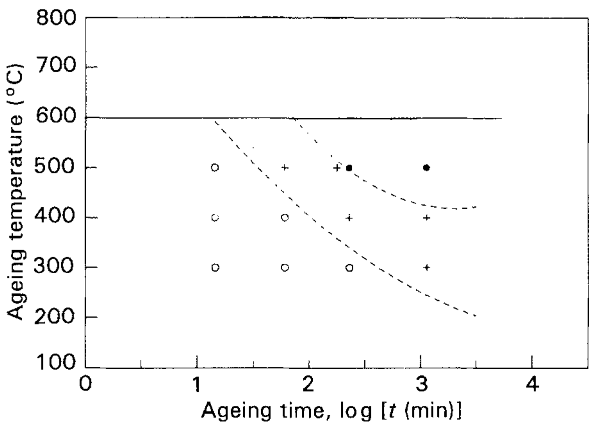

Figure 6 T–T–T diagram of precipitate transformation: (○) $Ti_{11}Ni_{14}$, (+) Ti_2Ni_3, (●) $TiNi_3$.

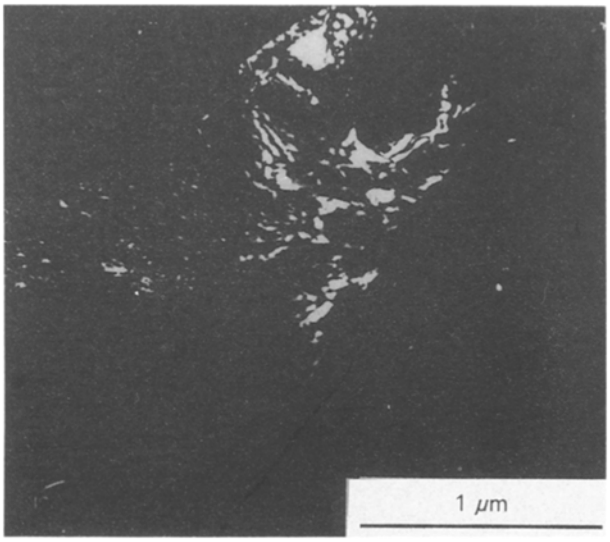

Figure 7 Dark-field image of specimen after 300 °C/15 min ageing treatment.

3.3. The ageing effect on M_s temperature

The effect of ageing temperature on the M_s temperature is shown in Fig. 10. For ageing temperatures 100 and 200 °C the M_s temperature does not change. This is because at low temperatures, precipitation hardly occurs, and the ordering of the atomic arrangement stays the same. For 300 and 400 °C, M_s decreases. This is due to the same factor that gives rise to the increase in hardness, i.e. coherent precipitates. For 500 °C, M_s increases, since over-ageing results in a loss of coherency and the Ni content in the matrix goes down. For 600 °C, M_s is nearly the same as for solution treatment since the temperature is now above the soluvs line.

The ageing time effect on the M_s temperature is shown in Fig. 11. For 300 and 400 °C, M_s initially decreases before it gradually increases again as the ageing time increases. For 500 °C, M_s steadily increases. These changes can be explained using the same account of coherency as detailed in the section on hardness. When the hardness is at its maximum, coherency prevails and drops to its minimum. After the coherency is disrupted, the Ni content in the matrix will drop and lead to a rise of M_s.

3.4. Comparison of the effects of constraint and no constraint on M_s

A comparison of the effects of constraint ageing and no-constraint ageing on M_s is shown in Fig. 12. Preferred precipitates form when constraint ageing is performed. A residual shear stress will remain on the interface between matrix and precipitate when the constraint is removed. As can be inferred from thermodynamic theory, the residual shear stress functions in the same way as applied stress in terms of its effect on M_s, which is to cause M_s to rise. Furthermore, the residual shear stress increases with the degree of preferred precipitation induced by the constraint stress. Therefore, the larger the constraint stress, the higher the M_s temperature.

3.5. Constraint ageing effect on stress required to induce martensite

A schematic representation of a stress–strain curve showing pseudo-elastic behaviour is shown in Fig. 13.

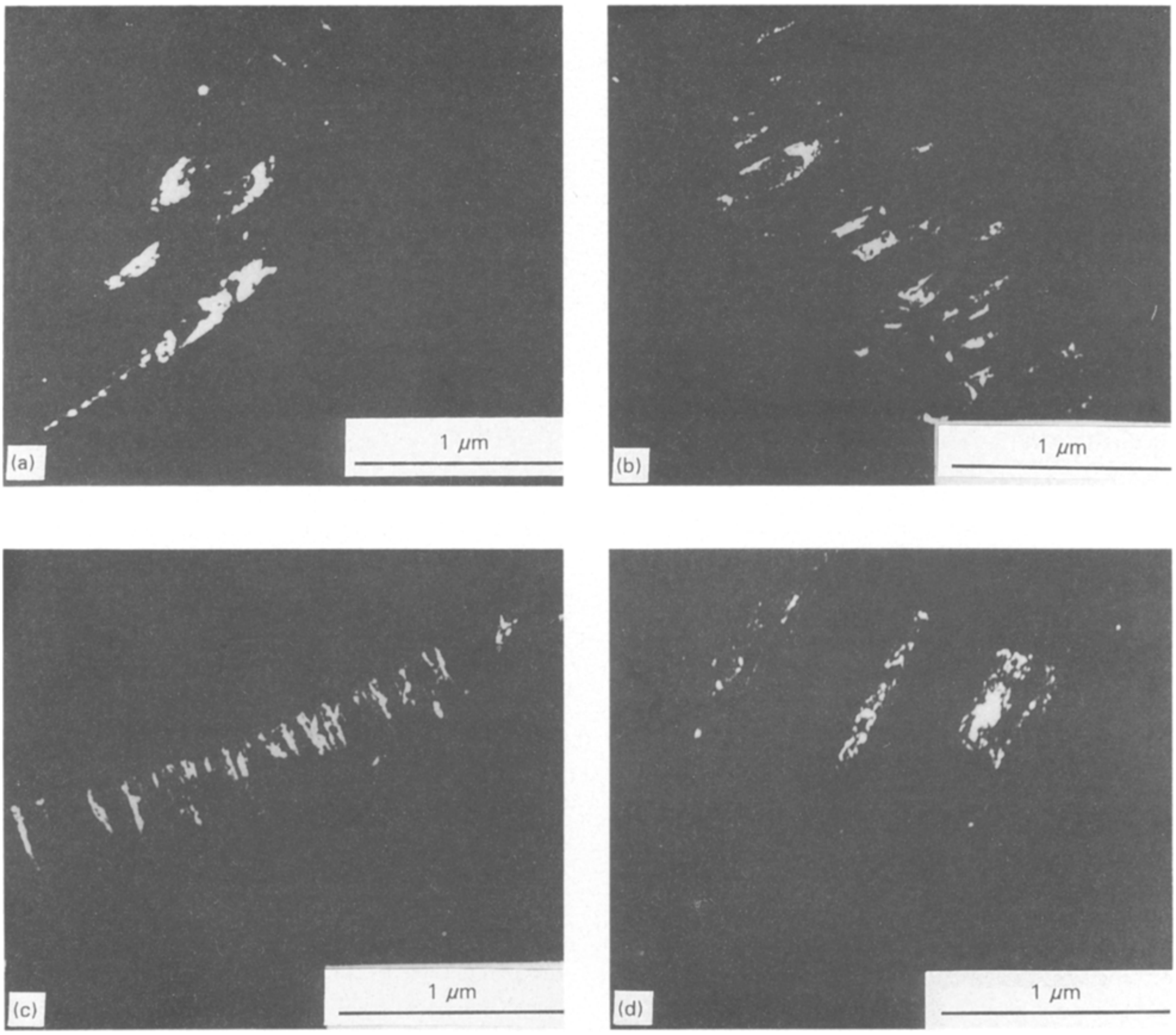

Figure 8 Dark-field images of 50 MPa constraint-aged specimens: (a) 500 °C/15 min, (b) 400 °C/15 min, (c) 300 °C/15 min, (d) 400 °C/1 h.

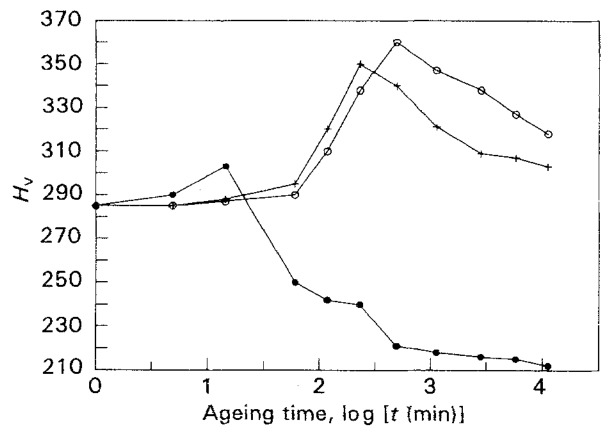

Figure 9 Curves for Vickers hardness corresponding to various ageing conditions: (○) 300 °C, (+) 400 °C, (●) 500 °C.

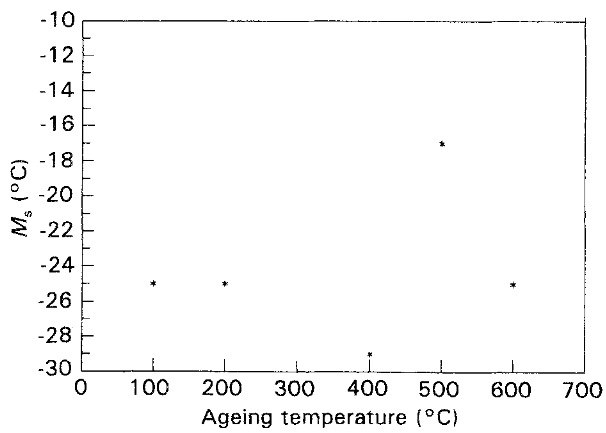

Figure 10 Effect of ageing temperature on M_s.

The yield stress can be quantitatively related to the M_s shift through the Clausius–Clapeyron equation:

$$\frac{d\sigma_{0.2}}{dT} = \frac{\Delta H \rho}{\varepsilon T_0}$$

where $\sigma_{0.2}$ is the applied stress at which stress-induced martensite is formed at testing temperature T, ρ the density, ΔH the enthalpy change of transformation and ε the strain corresponding to complete transformation.

From the above equation, the applied stress $\sigma_{0.2}$ changes with temperature difference (difference between T_0 and deformation temperature). Scheil [10] pointed out as early as 1932 that the stress required to

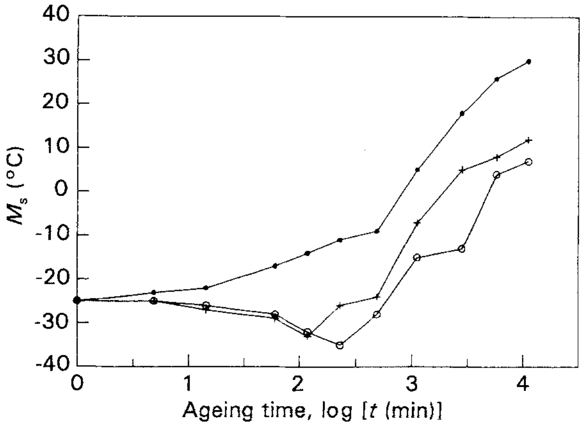

Figure 11 Effect of ageing time on M_s temperature: ageing temperature (○) 300 °C, (+) 400 °C, (●) 500 °C.

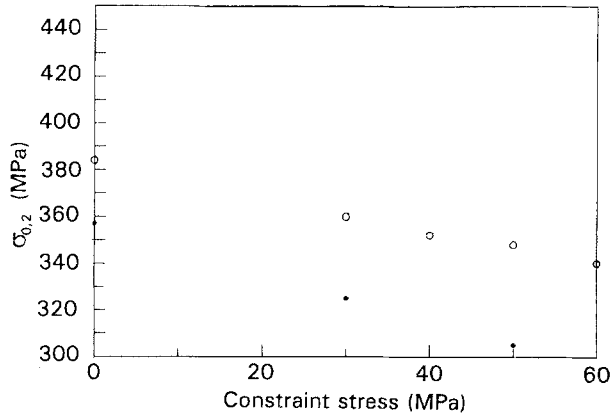

Figure 14 Effect of constraint stress on $\sigma_{0.2}$: ageing time (○) 15 min (●) 1 h.

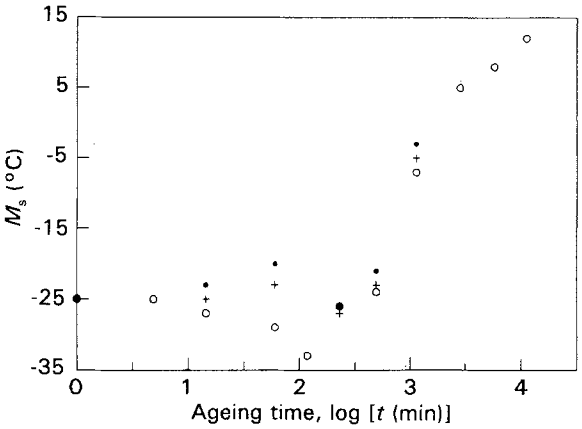

Figure 12 Effect on constraint ageing stress on M_s: (○) no constraint, (+) 30 MPa, (●) 50 MPa.

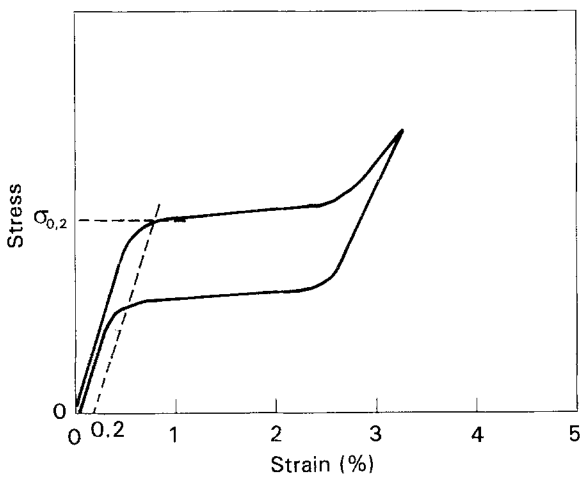

Figure 13 Schematic representation of a stress–strain curve showing the pseudoelastic behaviour.

induce a martensitic transformation decreased with decreasing temperature to become zero at M_s. The applied stress $\sigma_{0.2}$ is therefore changed by M_s. In general, the value of $d\sigma_{0.2}/dT$ is small. Except for the case when the temperature difference is large, the difference in $\sigma_{0.2}$ is negligible. Since the M_s temperature difference is small in our experiments, the effect of M_s change on applied stress $\sigma_{0.2}$ can be discounted.

It is now understood that martensitic transformation can be induced by the application of stress (the influence of shear stress is dominant) as well as by changes in temperature. The nucleation and growth of martensites are associated with shear strains and can be activated by stresses applied to the specimen. Moreover, the martensitic transformation is strongly dependent on the directions of stresses with respect to the lattice orientation. Honma [11] pointed out that constraint ageing would cause the $Ti_{11}Ni_{14}$ precipitate in Ni–Ti alloy to grow along the $[1\,1\,1]_{B2}$ direction. Therefore, the same direction is also presumed for the growth of $Ti_{11}Ni_{14}$ in our experiments. It then follows that residual shear stress fields will build up along $[1\,1\,1]_{B2}$ at the interface between the matrix and the precipitate. Furthermore, the magnitudes of the shear stress fields increase with the constraint stress. These fields play a major role in promoting nucleation and growth of martensite along their direction, i.e. $[1\,1\,1]_{B2}$. Ono *et al.* [12] discovered that martensite would most easily nucleate and grow along $[1\,1\,1]_{B2}$ in Ni–Ti shape memory alloy. This finding actually lends importance to the direction $[1\,1\,1]_{B2}$, since it is the direction favoured both by preferred precipitation under constraint ageing and by the emergence of martensite. It can therefore be concluded that increased constraint stress will not only enhance the resulting shear stress field but will promote the nucleation and growth of martensite as well. As a result, the stress required to induce martensite decreases as larger constraint stresses are applied. Fig. 14 demonstrates this effect.

4. Conclusions

The effects of constant-stress ageing on the shape memory properties of Ti–50.5 at % Ni have been investigated. The results are summarized as follows:

1. The precipitate sequence can be written as β_0 (Ti–Ni) → $Ti_{11}Ni_{14}$ → Ti_2Ni_3 → $TiNi_3$.

2. Precipitation hardening occurs in the 300 and 400 °C aged alloy. The M_s temperature of 300 and 400 °C aged Ti-50.5 at % Ni alloy is found to drop dramatically at first in the early ageing, to reach a minimum, and then to increase rapidly. At the same

time, the hardness is found to increase in the early ageing, reach a maximum, and then follow a monotonic decrease.

3. The constraint ageing treatment cause preferred orientation of precipitates to increase the M_s temperature and decrease $\sigma_{0.2}$.

References

1. K. OTSUKA and K. SHIMIZU, *Int. Met. Rev.* **31** (1986) (3) 93.
2. S. MIYAZAKI and K. OTSUKA, *ISIJ Int.* **29** (1989) 353.
3. D. GOLDSTEIN, L. KABACOFF and J. TYDINGO, *J. Metals* (March 1987) 19.
4. T. TADAKI, Y. NAKATA and K. SHIMIZU, *Trans. JIM* **28** (1987) 383.
5. T. SABURI, Y. TATSUMI and S. NENNO, *J. de Phys.* **43** (1982) c4–261.
6. M. NISHIDA and T. HONMA, *Scripta Metall.* **18** (1984) 1293.
7. *Idem, ibid.* **18** (1984) 1299.
8. T. TADAKI, Y. NAKATA, K. SHIMIZU and K. OTSUKA, *Trans. JIM* **27** (1986) 731.
9. M. NISHIDA, C. M. WAYMAN and T. HONMA, *Metall. Trans.* **17A** (1986) 1505.
10. E. SCHEIL, *Z. Anorg. Allg. Chem.* **207** (1932) 21.
11. T. HONMA, ICOMAT-86 (1986) 709.
12. N. ONO, A. SATOH and H. OHTA, *J. Jpn Inst. Met.* **50** (1986) 1049.

Received 24 September 1992
and accepted 8 June 1993